GRZEGORZ CIEPLOK [*], MARIAN SIKORA [*]

TWO-MASS DYNAMIC ABSORBER OF A WIDENED ANTIRESONANCE ZONE

Attempts to perform synthesis of a passive vibroinsulation two-mass system intended for the simultaneous reduction of machine frame vibrations and forces transmitted to foundations by supporting elements were undertaken in the study. In view of the variable frequency of the machine operation, it was necessary for the frequency interval, encompassed by the vibroinsulation system operation, to be within given limits. On the grounds of properties of the linear massive-elastic system formulated in the works of Genkin and Ryaboy (1998), the problem of vibroinsulation system synthesis was formulated in the parametric type optimisation approach with equality and inequality limitations. For piston compressor vibroinsulation, the mass and elasticity matrices of the vibroinsulating system, as well as its physical structure, were determined. Its operation was verified on the basis of simulation investigations, taking into account the system loss and transient states.

1. Introduction

The tasks of limiting forces transmitted to foundations by vibrating machines and devices, while taking into consideration human and environmental protection as well as legal regulations, are still very important. Piston machines can serve as an example since, due to their reciprocating motion, they constitute a source of vibrations perceived as annoyance by the surroundings, especially in large-scale units. In compressors applied in compressor stations, the connected pipeline transfers vibrations at long distances and is itself endangered by fatigue type defects.

A classic vibroinsulation application does not always provide the required results and is not always possible. Machine placement on elastic systems admittedly decreases force values transmitted by supporting elements to the

[*] AGH University of Science and Technology, A. Mickiewicza 30, 30-059 Krakow, Poland; E-mail: cieplok@agh.edu.pl, ms.abc@wp.pl

foundation, however, it leads to an increase in the machine frame vibration amplitude. In several cases this increase is inadmissible. For instance, vibrations of precise machines in the tobacco industry are not permitted to exceed allowable values determined by the producer.

The conflict between decreasing forces transmitted into the foundations and increasing vibration amplitudes occurring in classic vibroinsulation can be solved, in certain cases, by the application of passive systems e.g. a dynamic eliminator of vibrations (Czubak 2007, Dahlbe 1989, Flaga 2008 and Hartog 1947) or the DAVI dynamic anti-resonance vibroinsulation system (Flanelly 1967, Michalczyk 2001). In the first case, as a result of adding an elastic element loaded with an additional mass to the vibrating machine frame, the generation of the counterforce towards the exciting force is possible. This leads to a significant decrease in frame vibrations and forces transmitted to the foundation. Theoretically, for an undamped eliminator, it is possible to stop the frame motion (Harris' Shock and Vibration Handbook 6th.Ed. (2009) pages 198-231). However, this solution has a fundamental fault. The frequency interval, at which the amplitude and forces transmitted to the foundation are reduced, is – in relation to the operating frequency of the machine – quite small and surrounded by resonance frequencies – Fig. 1. This type of solution can be applied only in the case of drives of a constant operating frequency.

Solutions using dynamic anti-resonance vibroinsulation introduce additional forces in between the vibroinsulated object and the foundation. These forces are opposite phase forces but equal to the ones transmitted by a classic vibroinsulating system. In the case of a lever (Flanelly 1967) or oil-rubber vibroinsulator (Michalczyk 2001), the coefficient of the force transmission function is of an anti-resonance frequency, which does not have any resonance from the side of higher frequencies – Fig. 2. This type of solution is safer when the dynamic eliminator is applied, since fluctuations of the machine operating speed are not threatened by entering the resonance zone. In comparison with classic vibroinsulation, they ensure a higher dynamic stiffness in addition to which the coefficient of force transmission above the anti-resonance frequency leads asymptotically not to zero but to a constant value.

The task of synthesizing a vibroinsulation system (Dahlbe 1989, Genkin and Ryaboy 1988, Rade 2000), which would be able to meet the opposing properties of passive vibroinsulation, in other words: decreasing forces transmitted to the foundation by the supporting system and warranting a high dynamic stiffness of the vibroinsulated object mass in a sufficiently wide operating frequency interval of the device, was undertaken in the study.
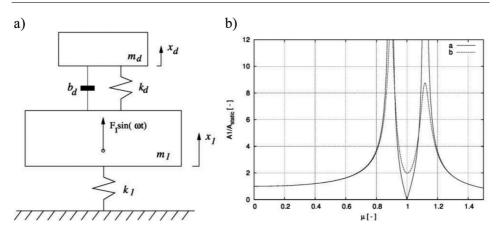
a)

b)

Fig. 1. Frahm dynamic eliminator. a) Sketch of the system b) Characteristics of vibration amplitude, (a) – without damping, (b) – with damping; $\mu = \omega/\omega_0$, $\omega_0 = \sqrt{k_1/m_1}$, $A_{static} = m_1 g/k_1$, A_1 – amplitude vibration of mass m_1 [11]
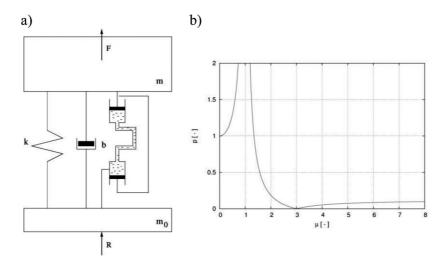
a)

b)

Fig. 2. DAVI type oil-rubber vibroinsulator. a) Sketch of the system. b) Characteristics of coefficient force transmissions $p = A_F/A_R$, where: A_F, A_R – amplitudes of forces F and R in sinusoidal steady state, $\mu = \omega/\omega_0$, $\omega_0 = \sqrt{k/m}$ [11]

2. Concept of building a multi-mass vibroinsulating system

The method of synthesis of multi-mass passive vibroinsulating systems is presented in the work by Genkin and Ryaboy (1988). As a result of increasing the number of degrees of freedom by widening its mechanical structure, the possibility of shaping the selected frequency characteristics can be achieved. This mainly concerns the coefficient of force transmission $p(\omega)$ (Fig. 3), which expresses the ratio of the amplitude of excitation forces F_1 causing

the system movement to the force amplitude transmitted to the foundation $R_{\max}(\omega)$ by the supporting elements:

$$p(\omega) = \frac{R_{\max}(\omega)}{F_1} \tag{1}$$

and the dynamic flexibility $G(\omega)$, understood as the ratio of the vibroinsulating mass displacement amplitude $A_{x1}(\omega)$ to the excitation force amplitude F_1:

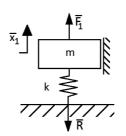$$G(\omega) = \frac{A_{x1}(\omega)}{F_1} \tag{2}$$

Fig. 3. The model of vibroinsulating mass excited by external force

These two parameters are especially essential when vibroinsulating systems are considered. A high value of the force transmission coefficient could cause damage to the foundation, building and could disturb other machine work. A high value of dynamic flexibility is responsible for high vibration amplitude of the body machine. This is the reason for damage to the machine, especially precision machines.
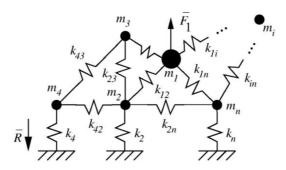
We consider the system shown in Fig. 4.

Fig. 4. Pictorial diagram of a multi-mass passive vibroinsulating system

The set of n material points is connected by some system of linear elastic elements. Some of these masses are connected directly to the ground, some

to the mass m_1, others are linked to each other. The mass m_1 is treated with special attention, because it represents the vibroinsulating object subjected to the vibration by the external force F_1. The equation of motion of the material points shown in Fig.4 takes the form:

$$[M]\frac{d^2}{dt^2}\bar{X}(t) + [K]\bar{X}(t) = \bar{F}_1(t) \tag{3}$$

where:

$[M] = \text{diag}(m_1, m_2, \ldots, m_n)$ – mass matrix,
$[K]$ – stiffness matrix,
$\bar{X}(t)$ – mass displacement vector,
$\bar{F}_1(t) = [F_1, 0, ..., 0]$ – force excitation vector,
$\bar{R}$ – ground reaction.

If we assume the excitation force impact on the mass m_1 is harmonic:

$$F_1(t) = F_1 \sin(\omega t) \tag{4}$$

and the response system in the steady state is:

$$\bar{X}(t) = \bar{X} \sin(\omega t) \tag{5}$$

then equation (3) assumes the form:

$$[K]\bar{X} - \omega^2[M]\bar{X} = \bar{F}_1 \tag{6}$$

This allows the calculation of the mass displacement vector m_i:

$$\bar{X} = \left\{[K] - \omega^2[M]\right\}^{-1} \bar{F}_1 \tag{7}$$

Based on d'Alembert's principle, we can write the equation resulting from the balance of active, reaction and inertia forces:

$$-R + \sum_{i=1}^{n} \omega^2 m_i X_i + F_1 = 0 \tag{8}$$

After adding rows of the matrix to equation (6), and taking equation (8) into account, we obtain:

$$R = \sum_{i=1}^{n} \sum_{j=1}^{n} k_{ij} x_j \tag{9}$$

In matrix notation, (9) takes the form:

$$R = \bar{e}^T[K]\bar{X}, \quad \bar{e}^T = [1, 1, ..., 1] \tag{10}$$

Assuming excitation force as $F_1 = 1$, we obtain the displacement vector from (7):

$$\bar{X} = \left\{[K] - \omega^2[M]\right\}^{-1} \bar{e}_1, \quad \bar{e}_1 = [1, 0, ..., 0] \tag{11}$$

and the **force transmission coefficient**:

$$p(\omega) = \frac{R}{1} = \bar{e}^T[K]\left\{[K] - \omega^2[M]\right\}^{-1}\bar{e}_1 \tag{12}$$

The equation for the static displacement under the force $\bar{F}_1(t) = \bar{F}_{10}$ is:

$$[K]\bar{X}_0 = \bar{F}_{10} \tag{13}$$

From equation (13) above we can obtain $\bar{X}_0$:

$$\bar{X}_0 = [K]^{-1}\bar{F}_{10} = [D]\bar{F}_{10} \tag{14}$$

in the expanded form:

$$\begin{bmatrix} x_{10} \\ x_{20} \\ ... \\ x_{n0} \end{bmatrix} = \begin{bmatrix} d_{11} & d_{12} & ... \\ d_{21} & ... & ... \\ ... & ... & ... \\ d_{n1} & ... & d_{nn} \end{bmatrix} \begin{bmatrix} F_{10} \\ 0 \\ ... \\ 0 \end{bmatrix} \tag{15}$$

Considering the first line of the equality (15) we get:

$$x_{10} = d_{11}F_{10} \tag{16}$$

Finally, we obtain **the static stiffness** of the system k. This coefficient shows the ratio of the amplitude of the force F_{10} to the displacement of the mass m_1:

$$k = \frac{1}{d_{11}} = \frac{F_{10}}{x_{10}} \tag{17}$$

The considered system is in a uniform gravitational field with the value of acceleration g. The force $m_i g$ acts on each material point of the system, which can be represented in matrix notation:

$$\bar{F}_g = g[M]\bar{e} \tag{18}$$

If we replace in equation (14) the vector $\bar{F}_{10}$ by the vector $\bar{F}_g$ and displacement of the mass m_1 is denoted by Δ, then we get **the displacement of m_1 in a uniform gravitational field**:

$$\frac{\Delta}{g} = \bar{e}_1^T[D][M]\bar{e} \tag{19}$$

The dynamic flexibility can be obtained from equation (11). Based on the earlier assumption $F_1 = 1$ we obtain:

$$G(\omega) = \frac{x_1}{1} = \bar{e}_1^T \left\{ [K] - \omega^2[M] \right\}^{-1} \bar{e}_1 \tag{20}$$

Matrices $[M]$ and $[K]$ can be converted to a diagonal form based on the linear transformations (21) and (22).

$$[\Phi]^T[M][\Phi] = [E] \tag{21}$$

$$[\Phi]^T[K][\Phi] = [\Lambda] \tag{22}$$

where:

$[E]$ – identity matrix,

$[\Lambda] = \text{diag}[\omega_1^2, \omega_2^2, \ldots, \omega_n^2]$ – eigenfrequency squares matrix.

The transformation matrix $[\Phi]$ is composed of eigenvectors obtained from a non-trivial solution of equation (23):

$$\left([K] - \omega^2[M] \right) \bar{\varphi}_i = 0 \tag{23}$$

We multiply equations (21) and (22) on the left by $[\Phi^T]^{-1}$ and on the right by $[\Phi]^{-1}$, obtaining:

$$[M] = [\Psi][\Psi]^T \tag{24}$$

$$[K] = [\Psi][\Lambda][\Psi]^T \tag{25}$$

where:

$$\{\Psi\} = (\{\Phi\}^T)^{-1}$$

Based on the relationship (24) and (25), we can write:

$$\left([K] - \omega^2[M] \right)^{-1} = [\Phi] \left([\Lambda] - \omega^2[E] \right)^{-1} [\Phi]^T \tag{26}$$

If we substitute formula (26) to equation (20) we get **the dynamic flexibility**:

$$G(\omega) = \bar{e}_1^T[\Phi] \left([\Lambda] - \omega^2[E] \right)^{-1} [\Phi]^T \bar{e}_1 = \sum_{j=1}^{n} \frac{\varphi_{1j}^2}{\omega_j^2 - \omega^2} \tag{27}$$

If we act as above, based on equations (12) and (26), we get **the force transmission coefficient**:

$$p(\omega) = \bar{e}^T[\Psi][\Lambda] \left([\Lambda] - \omega^2[E] \right)^{-1} [\Phi]^T \bar{e}_1 = \sum_{i=1}^{n} \frac{\varphi_{1i}\omega_i^2 \sum_{j=1}^{n} \psi_{ji}}{\omega_i^2 - \omega^2} \tag{28}$$

In the final forms of the dynamic flexibility and force transmission coefficient, we can see that some sets of parameters are repeated: φ_{1i} – component of the first row of the matrix $[\Phi]$, as well as $\sum_{j=1}^{n} \psi_{ji}$ row component vector consisting of the sum of rows of the matrix $[\Psi]$. To simplify formulas (27) and (28) we introduce the new vectors:

$$\bar{U} = \bar{e}_1^T [\Phi] \tag{29}$$

and:

$$\bar{V} = \bar{e}^T [\Psi] \tag{30}$$

Now, formulas (27) and (28) obtain the following forms:

$$G(\omega) = \sum_{i=1}^{n} \frac{u_i^2}{\omega_i^2 - \omega^2} \tag{31}$$

$$p(\omega) = \sum_{i=1}^{n} \frac{u_i v_i}{1 - \left(\frac{\omega}{\omega_i}\right)^2} \tag{32}$$

Using formula (31), we can obtain **the static flexibility** of the system as the function value $G(\omega)$ for the frequency $\omega = 0$:

$$d_{11} = \frac{1}{k} = \sum_{i=1}^{n} \frac{u_i^2}{\omega_i^2} \tag{33}$$

The use of vectors $\bar{U}$ and $\bar{V}$ also allows **the whole system mass** to be described:

$$\bar{V}\bar{V}^T = \bar{e}^T [\Psi][\Psi]^T \bar{e} = \bar{e}^T [M] \bar{e} = \sum_{i=1}^{n} m_i = m \tag{34}$$

The diagonal matrix of the inverse mass m_i is equivalent to the inverse of the mass matrix $[M]$, therefore:

$$\frac{1}{m_1} = \bar{e}_1^T [M]^{-1} \bar{e}_1 = \bar{e}_1^T ([\Psi][\Psi])^{-1} \bar{e}_1 = \bar{e}_1^T [\Phi][\Phi]^T \bar{e}_1 = \sum_{i=1}^{n} u_i^2 \tag{35}$$

Based on formula (19), we get **the displacement system in the uniform gravity field**:

$$\frac{\Delta}{g} = \bar{e}_1^T \left([\Psi][\Lambda][\Psi]\right) [\Psi][\Psi]^T \bar{e} = \bar{e}_1^T [\Phi][\Lambda]^{-1}[\Psi]^T \bar{e} = \bar{U}[\Lambda]^{-1}\bar{V}^T = \sum_{i=1}^{n} \frac{u_i v_i}{\omega_i^2} \tag{36}$$

The identity $[\Phi][\Psi^T] = [E]$ implies an additional dependence describing the vectors $\bar{U}$ and $\bar{V}$. If we multiply the elements of the first row of the matrix $[\Phi]$ by the sum of columns of the matrix $[\Psi]$, we get:

$$\bar{U} \circ \bar{V} = \bar{U}\bar{V}^T = \sum_{i=1}^{n} u_i v_i = 1 \qquad (37)$$

3. Model of the piston compressor

Let us consider Fig. 5, which presents a simplified piston compressor. The crank shaft operating speed, dependent on the gaseous factor demand, is contained within the range $280 \div 330\, rpm$. The mass of the vibrating part, equal to approx. 65000 kilograms, is placed on the foundation by means of a viscoelastic system. For the aims of comparison, the suspension parameters were selected in such a way as to correspond with classic vibroinsulation. The natural frequency of the vibroinsulated mass of 1 [Hz] is five times lower than the force frequency generated by the piston assembly movement. For such elastic suspension, the static deflection of the compressor frame resulting from the gravitational field of force equals approx. 248 [mm].
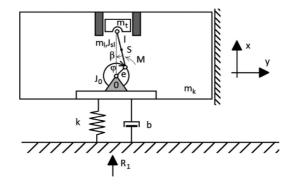

Fig. 5. Phenomenological model of the piston compressor. Parameters assumed for the analysis: $k = 2566100$ N/m, $b = 8170$ Ns/m, $m_k = 63836$ kg, $m_t = 776.1$ kg, $m_l = 388.1$ kg, $e = 0.168$ m, $l = 1.675$ m, $J_0 = 3700$ kgm^2, $J_{sl} = 90$ kgm^2. Power rating of the driving engine: $P_n = 1.8$ MW, transmission ratio: engine – driving shaft: $i = \frac{75}{33}$

Based on the Lagrangian function (38) of the considered system

$$L \cong E_k - E_p = \left(\frac{1}{2}m_k\dot{x}^2 + \frac{1}{2}J_0\dot{\varphi}^2 + \frac{1}{2}m_t(\dot{x} - e\sin(\varphi)\dot{\varphi})^2 + \frac{1}{2}m_l((\dot{x} - e\sin(\varphi)\dot{\varphi})^2 +$$
$$+ (\frac{1}{2}e\cos(\varphi)\dot{\varphi})^2) + \frac{1}{2}J_{ls}(\frac{e}{l}\cos(\varphi)\dot{\varphi})^2\right) - \left(\frac{1}{2}kx^2 + (m_t + m_l)\,ge\cos\varphi\right)$$

$$(38)$$

dynamic equations of motion can be obtained in the form:

$$
\begin{bmatrix}
1 & 0 & 0 & 0 \\
0 & 1 & 0 & 0 \\
0 & 0 & m_k + m_l + m_t & -(m_l + m_t)\sin(\varphi)e \\
0 & 0 & -(m_l + m_t)\sin(\varphi)e & J_0 + (m_l + m_t)\sin^2(\varphi)e^2 + \frac{1}{3}m_l\cos^2(\varphi)e^2
\end{bmatrix}
\frac{d}{dt}
\begin{bmatrix}
x \\
\varphi \\
v_x \\
\omega
\end{bmatrix}
=
$$

$$
=
\begin{bmatrix}
v_x \\
\omega \\
(m_l + m_t)\cos(\varphi)e\omega^2 - b\dot{x} - kx \\
M - (\frac{1}{3}m_l + \frac{1}{2}m_t)\sin(2\varphi)e^2\omega^2 - (m_l + m_t)eg\sin(\varphi)
\end{bmatrix}
$$

(39)

On the basis of this system, the simulations of the starting phase and steady state of the device were performed. The examples of machine body vibration and reaction force are shown in Fig. 6. The vibration amplitude of the compressor frame in the steady state achieved 3.1 [mm], while the amplitude of a
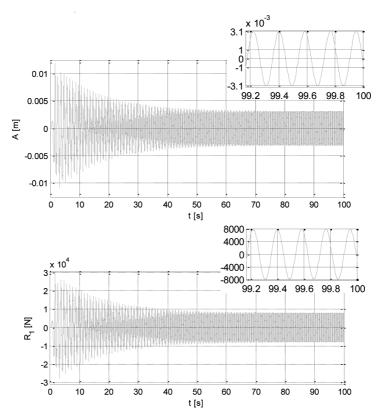

Fig. 6. Time-history of the coordinate $x(t)$ of the compressor frame mass centre and the force exerted on the foundation

variable component of force exerted by the supporting elements on the foundation was approx. 8 [kN]. In the starting phase, these were higher: 12 [mm] and 30.5 [kN] respectively. The values of the coefficient of force transmission and dynamic flexibility for the operating frequency can be determined on the basis of:

$$p = \frac{8000\,[\text{N}]}{P_0\,[\text{N}]} = 34.4 \cdot 10^{-3} \tag{40}$$

$$G = \frac{0.0031\,[\text{m}]}{P_0\,[\text{N}]} = 1.33 \cdot 10^{-8}\,[\text{m/N}] \tag{41}$$

where:

$$P_0 = (m_l + m_t)e\omega_r^2 = (388.1 + 776.1) \cdot 0.1675 \cdot 34.55^2 = 232\,776\ [\text{N}] \tag{42}$$

amplitude of the piston assembly force.

4. Synthesis of the vibroinsulation system

According to the method, the synthesis of a vibroinsulation system composed of massive and elastic elements can be performed in three stages.

In the first one, based on the assumptions concerning the vibroinsulation properties, the optimisation task is solved. In this optimisation, the objective function or functions (for example, coefficient of force transmission and/or dynamic flexibility) should obtain extreme values in the operating frequency interval of the device. The optimisation task can be made more specific by additional dependencies, which should be treated as equality or inequality limitations imposed on the task. First of all, the possibility of declaring the mass of the vibroinsulated object (35), the limitation of the object static deflection (36) and limitation of the mass of the synthesised vibroinsulation system (34) – dependencies, should be mentioned.

In the second stage, on the grounds of the obtained solutions $(\overline{U}, \overline{V}, \omega_i)$ and existing dependencies between the modal matrix rows, the complete form of the modal matrix $[\Phi]$ is determined and then – on its basis – the mass matrix $[M]$ and the elasticity matrix $[K]$ are determined.

Details of the algorithm for creating the matrices $[\Phi]$, $[M]$ and $[K]$ can be found in [6] on page 123.

In the third stage, on the grounds of the elasticity matrix $[K]$, the structure of the physical system is revealed. Since this process can be carried out in various ways, the system structure can take different forms. However, in general, the technique based on shaping the potential energy (43) of the system into a sum of potential energies V_i of components being reflected in the simple mechanical sub-assemblies is applied.

$$V = \sum V_i = \frac{1}{2}\bar{x}^T [K]\,\bar{x} \tag{43}$$

The sub-assembly shown in Fig. 7 can serve as an example. Its potential energy can be written in the form:

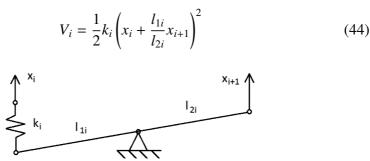$$V_i = \frac{1}{2}k_i\left(x_i + \frac{l_{1i}}{l_{2i}}x_{i+1}\right)^2 \tag{44}$$

Fig. 7. Lever sub-assembly

The presented approach adapted for determination of the vibroinsulation system – for the compressor described in Chapter 3 – can assume the equation system (45). The first dependence (45a) determines two objective functions – the coefficient of force transmission and dynamic flexibility, which their maximum values in the given operating frequency interval $[\omega_a, \omega_b]$ are minimised. Formally, this problem assumed the form of the multi-optimisation task, minimax type. In consideration of the significant differences in function values within the discussed frequency zone, the introduction of the balance coefficient α seems justified. Thus, the given function emphasized in the computational process depends on the value of this coefficient. On account of this, the results of three variants which, due to the balance parameter α, emphasise: coefficient of force transmission, dynamic flexibility and both functions with a similar significance – respectively, are presented in the paper. Successive dependencies of the system marked as (45b), (45c), (45d), (45e) determine, in the order of occurrence:

1. Declaration of vibroinsulated mass m_1. In the considered case: 65000 kilograms.
2. Ratio of the total mass of the system to the vibroinsulated mass. This was determined by the inequality relation and, according to the assumed parameter, $c_m = 1.2$, the mass of the added part cannot exceed 20% of the system mass.
3. Static displacement of the compressor mass in the gravitational field of force. Parameter $c_g = 1.02 \cdot 10^{-2}$, occurring also in the inequality dependence prevents displacements larger than 10 cm.
4. Obligatory dependence being met by the coefficient of force transmission (32), (37) in the case of frequency equal to 0.

$$\begin{cases} \max\limits_{\omega\in(29,32;\,34,56)} \left[\begin{array}{c} \left| \sum\limits_{i=1}^{n} \dfrac{u_i v_i}{1 - \left(\frac{\omega}{\omega_i}\right)^2} \right| \\[3mm] \alpha \left| \sum\limits_{i=1}^{n} \dfrac{u_i^2}{\omega_i^2 - \omega_r^2} \right| \end{array} \right] \to \min & \text{(45(a))} \\[10mm] \sum\limits_{i=1}^{n} u_i^2 - \dfrac{1}{m_1} = 0 & \text{(45(b))} \\[6mm] \sum\limits_{i=1}^{n} u_i^2 \sum\limits_{i=1}^{n} v_i^2 - c_m \le 0 & \text{(45(c))} \\[6mm] \left| \sum\limits_{i=1}^{n} \dfrac{u_i v_i}{\omega_i^2} \right| - c_g \le 0 & \text{(45(d))} \\[6mm] \sum\limits_{i=1}^{n} u_i v_i = 1 & \text{(45(e))} \end{cases}$$

The system (45) constitutes non-linear equations. Their solution is possible due to the application of numerical methods. The results presented in Table 1 were obtained by means of the minimax function, part of the Matlab engineering packet. The results of the optimised objective functions in the considered operating frequency interval of the device are presented in Figs. 8a and 8b.

It can be seen that, in the first variant, we obtained the largest reduction in force transmitted to the foundation, at a slightly decreased amplitude of the compressor frame vibrations. The force was reduced approximately 570 times. In the second variant, the force was reduced only by 49%, while the vibration amplitude was decreased approx. 4 times. In the third variant, the force transmitted to the foundation was decreased approximately 35.7 times and vibrations by approx. 1/3. It should also be mentioned that static stiffness attained much higher values compared to classic vibroinsulation. In the first variant, the vibroinsulated mass displaced itself by 10.2 [mm], in the second by 5.5 [mm] and in the third by 8.5 [mm]. Comparing these results with the value given in Chapter 3, we can notice that this value was increased by 24, 45 and 29 times – respectively.

On the grounds of dependence (44) and the elasticity matrices $[K]$ (Table 1), the physical structures of the systems can be determined. Such a structure for the third variant is presented in Fig. 9.

Table 1.

	VARIANT I	VARIANT II	VARIANT III
U	$\begin{bmatrix} -5.816 & -37.093 & 11.348 \end{bmatrix} \times 10^{-4}$	$\begin{bmatrix} 19.334 & -5.891 & 33.614 \end{bmatrix} \times 10^{-4}$	$\begin{bmatrix} 26.342 & 17.509 & 23.19 \end{bmatrix} \times 10^{-4}$
V	$\begin{bmatrix} 70.13 & -266.23 & 46.94 \end{bmatrix}$	$\begin{bmatrix} 209.7 & -89.7 & 161.1 \end{bmatrix}$	$\begin{bmatrix} 220.35 & 161.0 & 59.33 \end{bmatrix}$
ω_1 [1/s]	9.81	8.66	8.9
ω_2 [1/s]	23.48	22.01	15.36
ω_3 [1/s]	1902	143.6	502.8
m_1 [kg]	65000	65000	65000
m_2 [kg]	785	12353	12852
m_3 [kg]	12215	647	147.9
K [N/m]	$\begin{bmatrix} 1.97 \cdot 10^{10} & -7.16 \cdot 10^{9} & 0 \\ -7.16 \cdot 10^{9} & 2.60 \cdot 10^{9} & -7.45 \cdot 10^{5} \\ 0 & -7.45 \cdot 10^{5} & 6.59 \cdot 10^{6} \end{bmatrix}$	$\begin{bmatrix} 9.87 \cdot 10^{8} & -2.57 \cdot 10^{8} & 0 \\ -2.57 \cdot 10^{8} & 6.87 \cdot 10^{7} & 3.70 \cdot 10^{5} \\ 0 & 3.70 \cdot 10^{5} & 2.9 \cdot 10^{5} \end{bmatrix}$	$\begin{bmatrix} 5.75 \cdot 10^{9} & -3.48 \cdot 10^{9} & 0 \\ -3.48 \cdot 10^{9} & 2.11 \cdot 10^{9} & 1.68 \cdot 10^{5} \\ 0 & 1.68 \cdot 10^{5} & 2.78 \cdot 10^{4} \end{bmatrix}$
$p(\omega)_{max}$	0.00175	0.51	0.028
$G(\omega)_{max}$	$1.91 \cdot 10^{-8}$	$5.12 \cdot 10^{-9}$	$1.38 \cdot 10^{-8}$

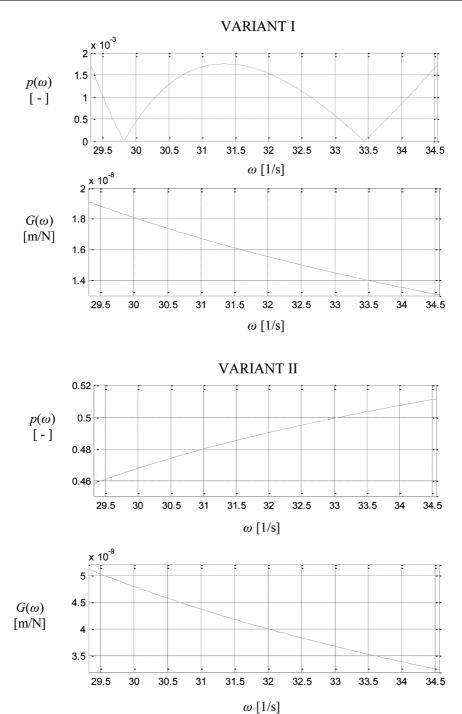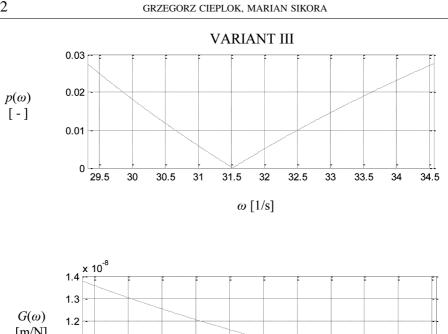## VARIANT I

VARIANT II

Fig. 8a. Diagrams of the coefficient of force transmission and dynamic flexibility in the compressor operating frequency interval, for variants I and II
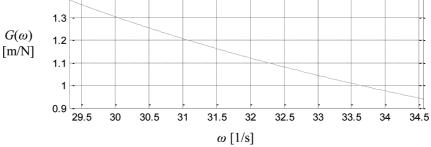
VARIANT III

Fig. 8b. Diagrams of the coefficient of force transmission and dynamic flexibility in the compressor operating frequency interval, for variant III
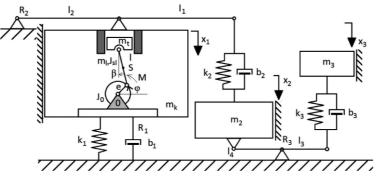

Fig. 9. Model of the compressor with the two-mass vibration absorber. Parameter values in the figure: $k_1 = 9.9 \cdot 10^6$ [N/m], $k_2 = 2.1 \cdot 10^9$ [N/m], $k_3 = 27.82 \cdot 10^3$ [N/m], $b_1 = 16.08 \cdot 10^3$ [Ns/m], $b_2 = 104.22 \cdot 10^3$ [Ns/m], $b_3 = 40.57$ [Ns/m], $\dfrac{l_1 + l_2}{l_2} = 1.65$, $\dfrac{l_3}{l_4} = 6.05$, $m_2 = 12852$ [kg], $m_3 = 147.9$ [kg]

5. Simulation investigations

When supplementing the compressor model by the vibroinsulating system, the Lagrangian function takes the form (46).

$$
\begin{aligned}
L = E_k - E_p = & \left(\frac{1}{2} m_k \dot{x}_1^2 + \frac{1}{2} J_0 \dot{\varphi}^2 + \frac{1}{2} m_t (\dot{x} - e \sin(\varphi)\dot{\varphi})^2 + \right. \\
& + \frac{1}{2} m_l ((\dot{x} - e \sin(\varphi)\dot{\varphi})^2 + (\frac{1}{2} e \cos(\varphi)\dot{\varphi})^2) + \frac{1}{2} J_{ls}(\frac{e}{l} \cos(\varphi)\dot{\varphi})^2 + \\
& + \frac{1}{2} m_2 \dot{x}_2^2 + \frac{1}{2} m_3 \dot{x}_3^2 \right) - \left(\frac{1}{2} k_1 x_1^2 + (m_t + m_l) \, ge \cos \varphi + \right. \\
& \left. \left. + \frac{1}{2} k_2 \left(x_2 - \frac{l_1 + l_2}{l_2} x_1 \right)^2 + \frac{1}{2} k_3 \left(x_3 - \frac{l_3}{l_4} x_2 \right)^2 \right) \right)
\end{aligned}
\tag{46}
$$

Based on it, we can obtain dynamic equations (47). On its basis, simulation investigations were carried out allowing the effectiveness of the solution and the system behaviour in transient states to be determined. As can be seen in Fig. 10, the application of a two-mass dynamic absorber allowed the amplitude of the compressor frame vibrations to be decreased to the value 2.2 [mm], which provided the vibration reduction by approx. 29%.
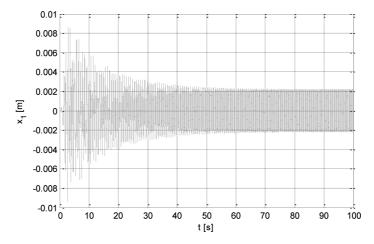

Fig. 10. Time-history of the compressor frame coordinate $x_1(t)$

$$
\begin{bmatrix}
1 & 0 & 0 & 0 & 0 & 0 & 0 & 0 \\
0 & 1 & 0 & 0 & 0 & 0 & 0 & 0 \\
0 & 0 & 1 & 0 & 0 & 0 & 0 & 0 \\
0 & 0 & 0 & 1 & 0 & 0 & 0 & 0 \\
0 & 0 & 0 & 0 & m_k + m_l + m_t & 0 & 0 & -(m_l + m_t)\sin(\varphi)e \\
0 & 0 & 0 & 0 & 0 & m_2 & 0 & 0 \\
0 & 0 & 0 & 0 & 0 & 0 & m_3 & 0 \\
0 & 0 & 0 & 0 & -(m_l + m_t)\sin(\varphi)e & 0 & 0 & J_0 + (m_l + m_t)\sin^2(\varphi)e^2 + \frac{1}{3}m_l\cos^2(\varphi)e^2
\end{bmatrix}
\frac{d}{dt}
\begin{bmatrix}
x_1 \\ x_2 \\ x_3 \\ \varphi \\ v_1 \\ v_2 \\ v_3 \\ \omega
\end{bmatrix}
=
$$

$$
=
\begin{bmatrix}
v_1 \\
v_2 \\
v_3 \\
\omega \\
(m_l + m_t)\cos(\varphi)e\omega^2 - k_1 x_1 - k_2(x_2 + \alpha_2 x_1)\alpha_2 - b_1\dot{x}_1 - b_2(\dot{x}_2 + \alpha_2\dot{x}_1)\alpha_2 \\
-k_2(x_2 + \alpha_2 x_1) - k_3(x_3 + \alpha_3 x_2)\alpha_3 - b_2(\dot{x}_2 + \alpha_2\dot{x}_1) - b_3(\dot{x}_3 + \alpha_3\dot{x}_2)\alpha_3 \\
-k_3(x_3 + \alpha_3 x_2) - b_3(\dot{x}_3 + \alpha_3\dot{x}_2) \\
M - (\frac{1}{3}m_l + \frac{1}{2}m_t)\sin(2\varphi)e^2\omega^2 + (m_l + m_t)eg\sin(\varphi)
\end{bmatrix}
\tag{47}
$$

Forces transmitted to the foundation are located in three places. In point R_1, which is the connection of the vibroinsulated mass suspension with the foundation, and in points R_2 and R_3, marking the lever support points. Time-histories of these forces determined by the dependencies (48), (49) and (50) are presented in Fig. 11, and their sum in Fig. 12.

$$
R_1 = b_1\dot{x}_1 + k_1 x_1 \tag{48}
$$

$$
R_2 = (\alpha_2 + 1)(b_2(\dot{x}_2 + \alpha_2\dot{x}_1) + k_2(x_2 + \alpha_2 x_1)) \tag{49}
$$

$$
R_3 = (\alpha_3 + 1)(b_3(\dot{x}_3 + \alpha_3\dot{x}_2) + k_3(x_3 + \alpha_3 x_2)) \tag{50}
$$

As can be seen, the total force in the steady state has been reduced more than 34 times and is equal to approx. 6.8 [kN]. This reduction is approx. 5% lower than the value resulting from the coefficient of force transmission, however, it is justified since it results from taking into account damping in equations of motion. The forces R_1, R_2, R_3 obtain the values 22 [kN], 33.5 [kN], and 5.15 [kN] respectively, which correspond to: 9.5%, 14.4% and 2.2% in relation to the force value generated by the motion of the compressor crank mechanism.
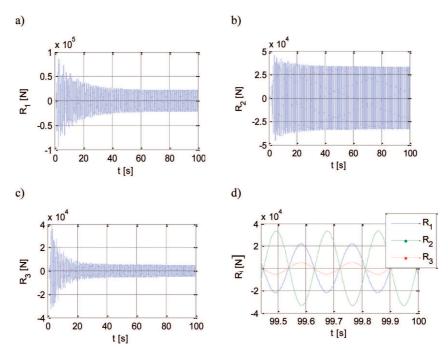
Fig. 11. Forces transmitted to the foundation by: a) point R_1, b) point R_2, c) point R_3, d) time-histories of forces in the steady state
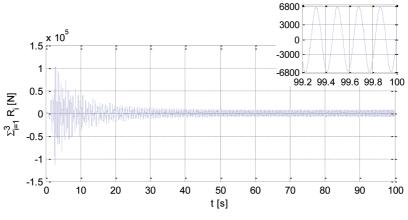

Fig. 12. Total force acting on the foundation

6. Conclusions

The results of the synthesis of a two-mass passive vibroinsulation system intended to reduce the negative effects of machine frame vibrations are presented in the paper. The vibroinsulating system's task was to decrease forces transmitted to the foundation and to lower machine frame vibration amplitudes in a relatively wide operating frequency interval. On account

of the low frequency of the excitation force of vibrating motion (from 4.6 [Hz] to 5.5 [Hz]), the classic vibroinsulation application, for which the static deflection would be approx. 250 [mm], was rejected. In order to achieve the best solution, an optimisation approach was applied in the synthesis.

Based on the analysis and simulation investigations presented in Sections 4 and 5, it can be observed that the set goals were achieved. While directing the objective function towards decreasing forces acting on the foundations, a force reduction by approximately 570 times was obtained, and in for directing this function towards decreasing the vibration amplitude a 4-time reduction was obtained. Such results in classic vibroinsulation would not be possible at all.

Less spectacular results were obtained in the case of variant 3, in which simultaneous minimisation of the force influence and amplitude lowering was required. Here, the force was reduced 34 times and vibrations by approx. 29%, for the piston operating frequency of 5.5 [Hz].

It should be mentioned that, in all three variants, the forces transmitted to the foundations are located in three places, which allows for a smoother distribution of loads on the foundation surface. In all variants, compared with classic vibroinsulation, several times lower static deflection was achieved. In the third variant it was only approx. 20 [mm].

The solutions obtained on the basis of the method are not flawless. Articulated joints and levers occur in such systems, and the number of degrees of freedom increases. However, it can be stated that, when limiting itself to passive systems, the method provides the best solutions in relation to the determination of the structure and optimal parameters of vibration reduction.

REFERENCES

[1] Czubak P.: Equalization of the Transport Velocity in a new Two-Way Vibratory Conveyor, Archives of Civil and Mechanical Engineering, vol. XI, 2011.

[2] Czubak P.: Analysis of a vibratory conveyor operating on the basis of the Frahm's eliminator of vibrations. Machine Dynamics Problems, vol. 31 no. 4, 2007.

[3] Dahlbe T.: On optimal use of the mass of a dynamic vibration absorber. Journal of Sound and Vibration 132, 1989.

[4] Flaga A., Szulej J., Wielgos P.: Comparison of determination methods of vibration's damping coefficient for complex structures. Budownictwo i Architektura 3, 2008.

[5] Flanelly W.G.: Dynamic anti-resonant vibration izolator. USA Patent No.3322379. Kaman Aircraft Corporation, 1967.

[6] Genkin M.D., Ryaboy V.M.: Elastic-Inertial Vibration Isolation Systems. Limiting Performance, Optimal Configuration (in Russian). Nauka, Moscow, 1988.

[7] Hadi M., Arfiadi Y.: Optimum design of absorber for MDOF structures. Journal of Structural Engineering, ASCE 1998; 124 (11): 1272-80.
[8] Hartog J.P.: Mechanical vibration, McGraw-Hill, New York, 1947.
[9] Mead Denys J.: Passive Vibration Control. John Wiley & Sons. England 2000.
[10] Michalczyk J., Czubak P.: Application of the antiresonant vibroinsulation in vibratory machines Machine Dynamics Problems, vol. 25, 2001.
[11] Michalczyk J., Cieplok G.: High-effective vibroinsulation and vibration attenuation systems. Collegium Columbinum, Krakow 1999.
[12] Rade D.A., Steffen V. Jr.: Optimisation of dynamic vibration absorbers over a frequency band, Mechanical Systems and Signal Processing 14, 2000.
[13] Whiteford G.P.: Multi-directional tuned vibration absorber. US Patent 6065742, 2000.
[14] Zuo L., Nayfeh S.A.: Minimax optimization of multi-degree-of-freedom tuned-mass dampers. Journal of Sound and Vibration 272, 2004.

Dwumasowy tłumik dynamiczny o poszerzonej kotlinie antyrezonansowej

S t r e s z c z e n i e

Praca podejmuje zadanie syntezy dwumasowego układu wibroizolacji pasywnej przeznaczonego do jednoczesnej redukcji drgań korpusu maszyny i sił przenoszonych przez elementy podparcia na konstrukcję wsporczą. Ze względu na zmienną częstotliwość pracy maszyny zażądano by przedział częstotliwości objęty działaniem układu wibroizolacji mieścił się w zadanych granicach. Opierając się na własnościach liniowych układów sprężysto masywnych sformułowanych w pracach Genkina i Ryaboya (1988) problem syntezy układu wibroizolacji sformułowano w ujęciu optymalizacyjnym typu parametrycznego z ograniczeniami równościowymi i nierównościowymi. Dla konkretnego przypadku, dotyczącego wibroizolacji sprężarki tłokowej, wyznaczono macierze mas i sprężystości ustroju wibroizolacyjnego, jego fizyczną strukturę oraz zweryfikowano działanie na podstawie badań symulacyjnych uwzględniających stratność układu i stany przejściowe.